Journal of Organometallic Chemistry, 384 (1990) 279–293
Elsevier Sequoia S.A., Lausanne – Printed in The Netherlands
JOM 20419

Antiferromagnetic complexes with metal–metal bonds

XX *. Synthesis, molecular structure, electronic structure and magnetic properties of the cyclopentadienyl-alkoxide complexes $Cp_2Cr_2(\mu\text{-}OR)_2[OCCo_3(CO)_9]$ and $Cp_2Cr_2(OR)_2(\mu\text{-}OR)_2$ ($R = CMe_3$)

S.E. Nefedov, A.A. Pasynskii *, I.L. Eremenko, B. Orazsakhatov, V.M. Novotortsev, O.G. Ellert, A.F. Shestakov,

N.S. Kurnakov Institute of General and Inorganic Chemistry, Academy of Sciences of the U.S.S.R., Leninsky prosp., 31, B-71 Moscow (U.S.S.R.)

A.I. Yanovsky, and Yu.T. Struchkov

A.N. Nesmeyanov Institute of Organoelement Compounds, Academy of Sciences of the U.S.S.R., Vavilov St., 28, B-312 Moscow (U.S.S.R.)

(Received September 5th, 1989)

Abstract

Interaction of the binuclear complex $Cp_2Cr_2(\mu\text{-}OCMe_3)_2$ (I) with $Co_2(CO)_8$ in the molar ratio 1/1 in benzene at room temperature yields the cluster $Cp_2Cr_2(\mu\text{-}OCMe_3)_2[OCCo_3(CO)_9]$ (II) (space group $P2_1/n$, a 10.377(4), b 17.879(7), c 18.115(7) Å, β 101.39(3)°, V 3294.7 Å^3, $Z = 4$, T −100 °C). One of the chromium atoms of the $Cp_2Cr_2(\mu\text{-}OCMe_3)_2$ fragment (Cr–Cr 2.766(1), Cr–$OCMe_3$ 1.950(3) Å) in complex II is bonded to the oxygen atom of the μ_3-CO group of the cluster fragment $Co_3(\mu_3\text{-}CO)(CO)_9$ (Cr–O 1.988(3), C–O 1.247(6) Å, Co–Co 2.483(1)–2.489(1) Å), which is an analogue of the alkoxide group. Compound II is treated as a $Cp_2Cr_2(OR)(\mu\text{-}OCMe_3)_2$ complex with chromium atoms of different oxidation states; its properties are compared with the characteristics of the binuclear tetraalkoxide $Cp_2Cr_2(OCMe_3)_2(\mu\text{-}OCMe_3)_2$ (III) which is formed along with the well-known cluster $Cp_4Cr_4Te_4$ in the reaction of I with tellurium. Complex III has been characterized by an X-ray diffraction study (space group $Pna2_1$, a 22.4539(12), b 11.7514(6), c 10.7303(5) Å, V 2831.3 Å, $Z = 8$, T 20 °C). Both Cr^{III} atoms of the binuclear fragment $Cp_2Cr_2(\mu\text{-}OCMe_3)_2$(Cr...Cr 3.004(3) Å, Cr–O(average) 2.000(9)

* For part XIX see ref. 16.

Å) in III are bonded to the terminal alkoxide group (Cr–O(average) 1.852(8) Å). Complexes I–III are antiferromagnetic. Calculations of the MOs for I–III compared with the well-known complex $Cp_2Cr_2(OMe)_2(NO)_2$ have been carried out by the extended Hückel method.

Introduction

The binuclear complex $Cp_2Cr_2(\mu\text{-}OCMe_3)_2$ (I) was first synthesized by Chisholm and Cotton and studied as a model of the active centre of an ethylene polymerization catalyst [1]. Another important feature of complex I is its antiferromagnetic properties ($-2J$ 246 cm^{-1}) [2] in combination with the short direct Cr–Cr bond (2.635 Å) [1]. It is noteworthy that the geometry of the Cp^*–Cr–Cr–Cp^* fragment (where Cp^* is the centroid of the C_5H_5 ligand; the Cp^*CrCr angles are equal to 143.9 and 146.3°) is not so favourable for σ-metal–metal bond formation as in the case of another antiferromagnetic complex, $Cp_2Cr_2(\mu\text{-}S)(\mu\text{-}SCMe_3)_2$ (II) ($-2J$ 430 cm^{-1}), which has a linear Cp^*–Cr–Cr–Cp^* group (Cr–Cr 2.689 Å) [3]. The situation changes considerably when the bridging $Fe(CO)_4$ fragment is attached to I: the $Cp^*CrCrCp^*$ group becomes linear and although the length of the Cr–Cr bond (2.635 Å) does not change, the parameter of antiferromagnetic exchange increases ($-2J$ 304 cm^{-1}) [2]. On the other hand, oxidative addition of terminal halogen atoms to the chromium atoms of I results in the formation of $Cp_2Cr_2(X)_2(\mu\text{-}OR)_2$ (X = Cl, Br, I) dimers with smaller Cp^*CrCr angles, less effective overlap of the d_{z^2} orbitals and corresponding weakening of the Cr–Cr bond (Cr...Cr 2.917–2.971 Å), which leads to a decrease of the parameter of antiferromagnetic exchange ($-2J$ 150–160 cm^{-1}) [4].

It seemed quite interesting to study the addition of the $Co(CO)_4$ fragment to complex I. Its geometry is similar to that of $Fe(CO)_4$, whereas its electronic function is analogous to that of a halogen atom: the $Co(CO)_4$ group readily adds one electron, forming the $[Co(CO)_4]^-$ anion. The addition to I of tellurium atom, which demonstrates carbenoid properties analogous to $Fe(CO)_4$, has also been studied.

Results and discussion

Interaction of $Cp_2Cr_2(\mu\text{-}OCMe_3)_2$ (I) with $Co_2(CO)_8$ occurs practically instantly in benzene at room temperature with the formation of a dark-crimson solution. On cooling, it yields large brown-crimson prisms of the cluster $Cp_2Cr_2(\mu\text{-}OCMe_3)_2$-$[OCCo_3(CO)_9]$ (II), which are extremely sensitive to atmosphere oxygen and moisture.

In the spectrum of I, a band at 1390 cm^{-1}, characteristic of the stretching vibrations of an isocarbonyl-type bridging CO group, is observed. According to the X-ray diffraction data (Fig. 1, Tables 1–3), molecule II preserves the binuclear fragment $Cp_2Cr_2(\mu\text{-}OCMe_3)_2$ (Cr–O(average) 1.950(3) Å) with a trinuclear cluster fragment $OCCo_3(CO)_9$ (Co–Co 2.483(1)–2.489(1) Å) bonded to one of the chromium atoms via the oxygen atom of the μ_3-bridging CO (Cr–O 1.988(3), μ_3-C–O 1.247(6) Å). As a result, quite different displacements of the C_5H_5-ligand centroids from the Cr–Cr axis (Cp^*CrCr 117.2 and 155.7°) are observed together with weakening of the metal–metal bond (2.766(1) Å). One may consider two points of

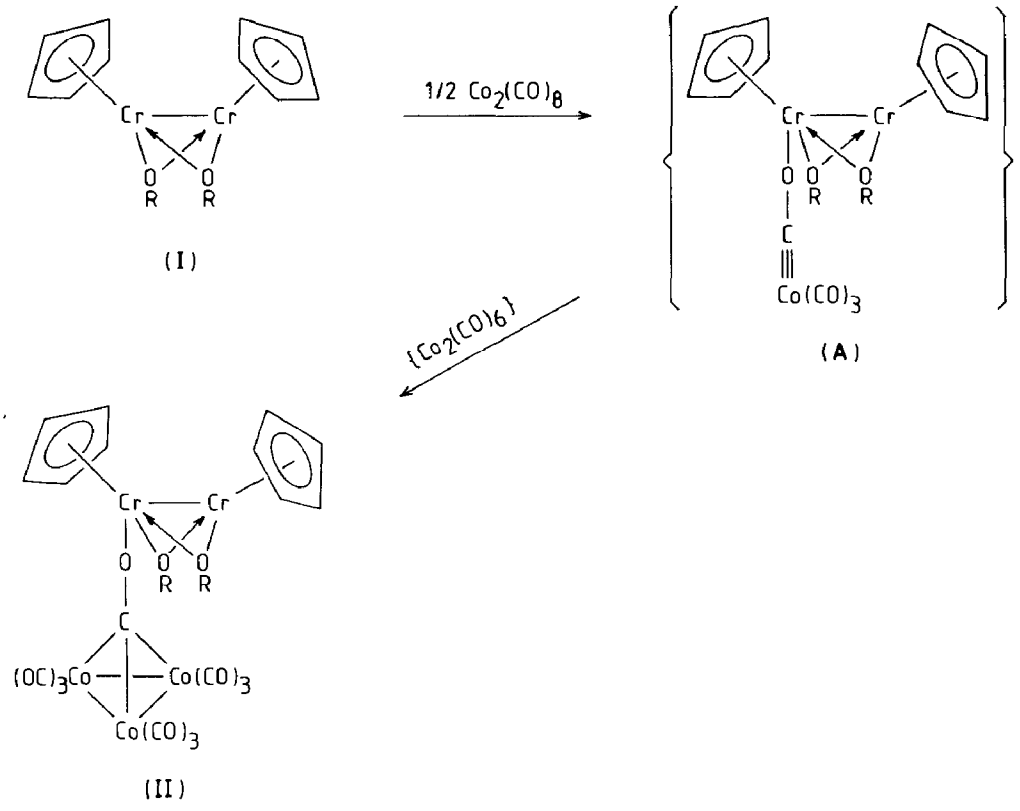

view on molecule II. On the one hand, the fragment $O[Cp_2Cr_2(\mu\text{-}OCMe_3)_2]$ may be regarded as a metal-containing group R in the well-known clusters of type $(CO)_9Co_3CR$ [5]. On the other hand, the trinuclear fragment $(CO)_9Co_3C$ may act as R′ in the tris-alkoxide complex $Cp_2Cr_2(OR')(\mu\text{-}OCMe_3)_2$, involving chromium atoms in different oxidation states: Cr^{II} and Cr^{III}. Complex II is antiferromagnetic and μ_{eff} per Cr atom decreases from 2.48 to 1.72 BM in the temperature range 296–77 K, which may be described by the dimeric Heisenberg–Dirac–Van Vleck model with the exchange parameter $-2J$ 164 cm^{-1} (the admixture of monomer is 6% with a mean square error of 1%).

It is noteworthy that II can be formed when the ratio of the reagents is different. One may assumed that in the first stage of interaction, oxidation of Cr^{II} to Cr^{III} with simultaneous conversion of $Co(CO)_4$ to $Co(CO)_4^-$ anion takes place. It is known that this anion adds hard Lewis acids (H^+, Cp_2Ln^+, etc. [6]) as a hard Lewis base via the carbonyl oxygen with the formation of the alkoxide-carbyne system $M{-}O{-}C{\equiv}Co(CO)_3$ in the intermediate complex A. Further, fast addition of the $Co_2(CO)_6$ fragment to the $Co{\equiv}C$ bond leading to $OCCo_3(CO)_9$ most probably takes place, as has been observed earlier in the case of the diamagnetic sandwich complexes $Cp_2M[OCCo_3(CO)_9]_2$ (M = Ti, Zr, Hf) [7].

On the other hand, the binuclear complex of Cr^{III} with four alkoxide groups, $Cp_2Cr_2(OCMe_3)_2(\mu\text{-}OCMe_3)_2$ (III), has been isolated in the reaction of I with tellurium metal.

At the same time, the well-known tetranuclear cluster $Cp_4Cr_4Te_4$ (IV) which gives a molecular ion in the mass spectrum, is formed. It is likely that an intermediate,

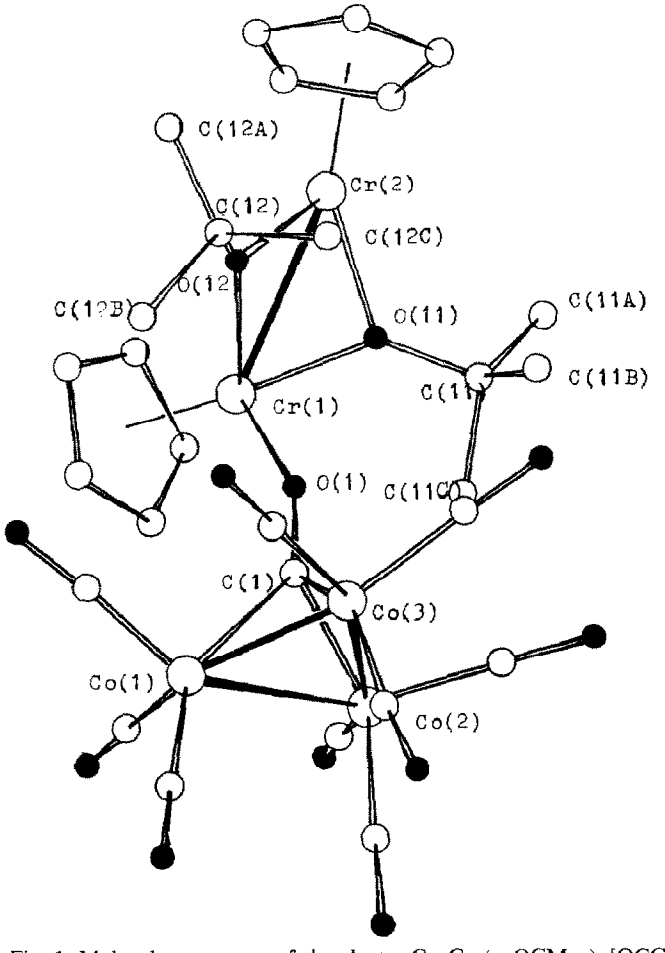

Fig. 1. Molecular structure of the cluster $Cp_2Cr_2(\mu\text{-}OCMe_3)_2[OCCo_3(CO)_9]$.

$(CpCrOCMe_3)_2Te$, analogous to the $(CpCrOCMe_3)_2Fe(CO)_4$ complex described above is formed:

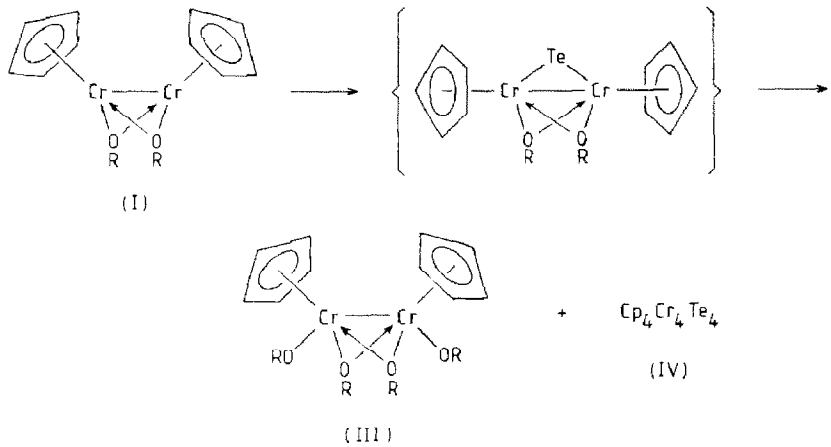

Table 1

Atomic coordinates of the cluster $Cp_2Cr_2(\mu\text{-}OCMe_3)_2[OCCo_3(CO)_9]$ (II) ($\times 10^5$ for Co and Cr; $\times 10^4$ for the others)

Atom	x	y	z
Co(1)	79053(7)	76683(4)	50422(4)
Co(2)	89134(7)	88217(4)	46372(4)
Co(3)	70717(7)	82028(4)	37689(4)
Cr(1)	110732(8)	71910(4)	34202(5)
Cr(2)	119494(8)	57461(5)	32835(5)
O(1)	9607(3)	7407(2)	3948(2)
O(2)	5675(5)	8212(3)	5674(3)
O(3)	9894(5)	7520(3)	6402(3)
O(4)	7290(6)	6081(2)	4782(3)
O(5)	9399(4)	9833(2)	3465(2)
O(6)	11585(4)	8850(2)	5522(3)
O(7)	7459(4)	9822(2)	5495(3)
O(8)	5016(4)	9205(2)	4158(2)
O(9)	5637(4)	6845(2)	3225(3)
O(10)	7394(4)	8731(2)	2292(2)
O(11)	10348(3)	6306(2)	2858(2)
O(12)	12061(3)	6467(2)	4120(2)
C(1)	8807(5)	7821(3)	4181(3)
C(2)	6546(6)	8017(3)	5430(4)
C(3)	9119(6)	7584(4)	5847(4)
C(4)	7522(7)	6695(4)	4872(4)
C(5)	9205(5)	9427(3)	3915(3)
C(6)	10519(5)	8813(3)	5183(3)
C(7)	8009(6)	9438(3)	5164(3)
C(8)	5803(5)	8823(3)	4003(3)
C(9)61	6196(5)	7373(3)	3437(4)
C(10)	7283(5)	8526(3)	2871(3)
C(11)	9021(5)	6070(3)	2554(3)
C(11A)	8240(5)	6752(3)	2216(3)
C(11B)	8443(6)	5731(3)	3179(4)
C(11C)	9068(6)	5506(3)	1936(3)
C(12)	12317(5)	6366(3)	4917(3)
C(12A)	13649(7)	6021(4)	5140(4)
C(12B)	11249(7)	5866(4)	5102(4)
C(12C)	12278(6)	7125(3)	5282(3)
C(13)	12912(5)	7857(3)	3450(3)
C(14)	11895(5)	8361(3)	3512(3)
C(15)	10914(5)	8315(3)	2844(3)
C(16)	11333(6)	7788(3)	2372(3)
C(17)	12537(5)	7498(3)	2738(3)
C(18)	12375(6)	4990(3)	2340(3)
C(19)	12157(6)	4527(3)	2923(4)
C(20)	13166(6)	4675(3)	3558(4)
C(21)	14002(6)	5216(3)	3349(3)
C(22)	13528(6)	5388(3)	2594(3)

Table 2

Bond lengths of the cluster $Cp_2Cr_2(\mu\text{-}OCMe_3)_2[OCCo_3(CO)_9]$ (II)

Bond	d (Å)	Bond	d (Å)
Co(1)–Co(2)	2.488(1)	Cr(1)–O(11)	1.950(3)
Co(1)–Co(3)	2.489(1)	Cr(1)–O(12)	1.954(3)
Co(2)–Co(3)	2.483(1)	Cr(2)–O(11)	1.963(3)
Co(1)–C(1)	1.990(5)	Cr(2)–O(12)	1.975(3)
Co(2)–C(1)	1.964(5)		
Co(3)–C(1)	1.933(5)		
C(1)–O(1)	1.247(6)		
Cr(1)–O(1)	1.988(3)		
Cr(1)–Cr(2)	2.766(1)		

III is readily soluble in organic solvents and can be isolated as large brown prisms on recyrstallization from heptane. The bonding of metal atoms in molecule III (Fig. 2, Table 4–6) with bulky terminal t-butoxyl groups (Cr–O 1.861(8)–1.843(8) Å) results in a considerable deviation of both Cp rings from the Cr–Cr axis (Cp^*CrCr 123.1°), thus hindering overlap of the d_{z^2} orbitals. As a result, the Cr–Cr distance is as long as 3.004(3) Å. Complex III demonstrates antiferromagnetic properties: μ_{eff} per Cr atom decreases from 2.83 to 1.40 BM in the temperature range 296–77 K.

The considerable shortening of the terminal $Cr–OCMe_3$ bonds (average 1.852 Å) in comparison with the bridging $Cr–OCMe_3$ bonds (2.000 Å) is noteworthy. The $Cr–OCMe_3$ terminal bonds are also shortened in comparison with the sum of the covalent radii of the Cr and O atoms (1.46 and 0.66 Å, respectively), which indicates the significant contribution of additional π-interaction of lone electron pairs of the oxygen atoms of the terminal alkoxide groups with the half-filled orbitals of the chromium atoms.

In order to interpret the observed effects and to evaluate the spin state of the chromium atoms, calculations of the energetic spectrum of the one-electron levels of

Table 3

Bond angles of the cluster $Cp_2Cr_2(\mu\text{-}OCMe_3)_2[OCCo_3(CO)_9]$ (II)

Angle	(°)	Angle	(°)
Co(2)Co(1)Co(3)	59.85(3)	Cr(2)Cr(1)O(11)	45.2(1)
Co(1)Co(2)Co(3)	60.09(3)	Cr(2)Cr(1)O(12)	45.6(1)
Co(1)Co(3)Co(2)	60.05(3)	O(11)Cr(1)O(12)	84.3(1)
Co(1)C(1)Co(2)	78.0(2)	Cr(1)Cr(2)O(11)	44.8(1)
Co(1)C(1)Co(3)	78.7(2)	Cr(1)Cr(2)O(12)	45.0(1)
Co(2)C(1)Co(3)	79.1(2)	O(11)Cr(2)O(12)	83.4(1)
Co(1)C(1)O(1)	129.2(4)	Cr(1)O(11)Cr(2)	89.9(1)
Co(2)C(1)O(1)	134.3(4)	Cr(1)O(12)Cr(2)	89.5(1)
Co(3)C(1)O(1)	135.2(4)		
Cr(1)O(1)C(1)	154.4(3)		
Cr(2)Cr(1)O(1)	121.4(1)		

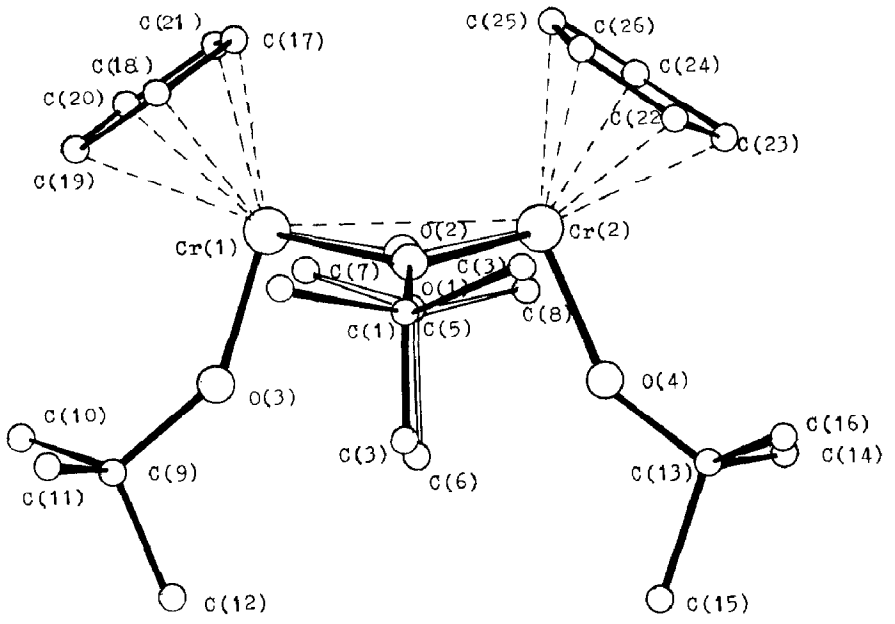

Fig. 2. Molecular structure of the binuclear complex $Cp_2Cr_2(\mu\text{-}OCMe_3)_2(OCMe_3)_2$.

complexes I–III were performed. The results were compared with those for the well-known diamagnetic complex $Cp_2Cr_2(\mu\text{-}OMe)_2(NO)_2$ (V) [8], in which the Cr atoms have the same coordination number (6) whereas the π-donor terminal OR groups are replaced by π-acceptor NO groups. The calculations were done by the extended Hückel method including a correction for the intra-atomic interaction of electrons * [10]. In order to simplify the calculations, the $OCMe_3$ groups in II and III and the tricobalt fragment $OCCo_3(CO)_9$ were replaced by OMe groups, as this does not in fact influence the energy of molecular orbitals of the *d*-block, which form the group of frontier orbitals (Fig. 3).

It should be noted that unambiguous classification of the orbitals to σ, π or δ types relative to the Cr–Cr bond was impossible because of the non-collinearity of the (C_5H_5-centroid)–Cr and Cr–Cr vectors in complexes I–III and V. Nevertheless, taking into account the stronger interaction of the Cr atoms with its ligand environment as compared to the Cr–Cr interaction, one may make an approximate assignment of the molecular orbitals to σ-, π- or δ-types according to their local symmetry relative to the (C_5H_5-centroid)–Cr axes. Index **A** for δ-type orbitals indicates that these orbitals are approximately antisymmetric relative to the plane passing through the Cr atoms and the C_5H_5 centroids. The Cr atoms in complex II are non-equivalent, which in some cases leads to different types of local symmetry and necessitates the use of more detailed designations (indices 1 and 2 refer to Cr atoms with coordination numbers 6 and 5, respectively). Figure 3 demonstrates the usual change of composition of the lowest bonding MO (transition from δ to σ symmetry) with an increase of the coordination number of Cr from 5 to 6, which

* Geometrical parameters were taken from the results of the X-ray diffraction study. Quantum-chemical parameters (ionization potentials and exponents) are listed in Table 7. The formula from ref. 9 was used for non-diagonal matrix elements.

Table 4

Atomic coordinates of the complex $Cp_2Cr_2(\mu\text{-}OCMe_3)_2(OCMe_3)_2$ (III) ($\times 10^5$ for Cr; $\times 10^4$ for the others)

Atom	x	y	z
Cr(1)	30939(8)	10912(18)	19405(0)
Cr(2)	38793(9)	31604(17)	19995(73)
O(1)	3578(4)	2027(7)	3179(9)
O(2)	3561(4)	1993(8)	755(9)
O(3)	3555(4)	−225(7)	1957(32)
O(4)	4666(3)	2715(7)	2044(28)
C(1)	3834(9)	1751(19)	4406(17)
C(2)	3924(11)	2760(17)	5163(15)
C(3)	4395(7)	895(15)	4050(17)
C(4)	3397(8)	993(20)	5100(14)
C(5)	3808(7)	1608(12)	−443(14)
C(6)	4349(7)	916(14)	−319(16)
C(7)	4072(9)	2786(16)	−1123(17)
C(8)	3265(8)	984(20)	−1106(18)
C(9)	3583(7)	−1480(10)	1742(28)
C(10)	4252(7)	−1779(13)	1712(53)
C(11)	3248(10)	−1907(13)	907(21)
C(12)	3311(11)	−1922(18)	3343(24)
C(13)	5293(6)	3072(13)	2081(48)
C(14)	5432(7)	3584(15)	658(21)
C(15)	5647(6)	1915(14)	1734(42)
C(16)	5439(9)	4001(19)	3058(22)
C(17)	2225(5)	2156(14)	2403(21)
C(18)	2227(7)	1706(19)	1134(22)
C(19)	2227(6)	621(15)	1102(19)
C(20)	2211(6)	94(16)	2236(50)
C(21)	2222(7)	1145(17)	3166(19)
C(22)	3606(9)	4763(8)	945(20)
C(23)	4090(7)	5070(10)	1808(51)
C(24)	3774(9)	4884(14)	3096(21)
C(25)	3192(8)	4506(13)	2421(22)
C(26)	3119(9)	4330(15)	1130(20)

leads, as stated above, to a decrease in the Cp*CrCr bond angle and a change in coordination of the local *d*-orbitals.

The results obtained show that the lowest *d*-block orbital (Table 8) makes the greatest contribution to the Cr–Cr bond population (0.094) in complex I. In II, this population is significantly smaller (0.053), and eventually in III and V it vanishes

Table 5

Bond lengths of the complex $Cp_2Cr_2(\mu\text{-}OCMe_3)_2(OCMe_3)_2$ (III)

Bond	d (Å)	Bond	d (Å)
Cr(1)–Cr(2)	3.004(3)	Cr(2)–O(2)	2.043(11)
Cr(1)–O(1)	2.038(9)	Cr(1)–O(3)	1.861(8)
Cr(1)–O(2)	1.960(10)	Cr(2)–O(4)	1.843(8)
Cr(2)–O(1)	1.958(11)		

Table 6

Bond angles of the complex $Cp_2Cr_2(\mu\text{-}OCMe_3)_2(OCMe_3)_2$ (III)

Angle	(°)	Angle	(°)
Cr(2)Cr(1)O(1)	40.2(6)	Cr(1)Cr(2)O(4)	109.4(6)
Cr(2)Cr(1)O(2)	42.4(5)	Cr(1)O(1)Cr(2)	97.4(1)
Cr(2)Cr(1)O(3)	110.2(6)	Cr(1)O(2)Cr(2)	97.2(1)
Cr(1)Cr(2)O(1)	42.2(6)		
Cr(1)Cr(2)O(2)	40.3(6)		

almost completely (0.032 and 0.030, respectively). In contrast to the other complexes of the series, the δ-orbitals of complex V are pushed out into the antibonding region, which is a result of the strong interaction of the NO group π^*-orbitals with the d_δ-orbitals of the Cr atoms (leading, however, to stabilization of the NO π^*-orbitals). The strengthening of this interaction is directly related to the π-acceptor properties of the NO ligand, as the NO π^*-orbital energy is closer to that of the Cr *d*-levels than the energy of the donor p_π-orbitals of the OR group.

In complex V, there are only two electrons in the MO with significant localization of the Cr atoms, although the main contribution of the total number of *d*-electrons comes from the filled orbitals, consisting of the bonding component of the NO π^*-orbitals and the Cr d_δ-orbitals.

Calculation of the energy levels ϵ_i and the populations of AOs in complexes I–III and V gives an opportunity to determine the local spins of paramagnetic Cr atoms within the model * of the local spin Hamiltonian [10] for the evalution of one-centre Coulomb interactions. However, it should be taken into consideration that because of the systematic errors of the theoretical model the accuracy of the determination of the total energy intervals does not exceed ~ 0.5 eV. As a result (Table 9), the most favourable spin states of the chromium atoms in I–III and V, in our opinion, are 3/2 and 3/2, 3/2 and 1, 3/2 and 3/2, and 1/2 and 1/2, respectively. Indeed, the magnetic properties of complexes I–III with these spin states of Cr atoms can be described within the dimeric model of Heisenberg–Dirac–Van Vleck [11] more satisfactorily than with other spin values (Table 10).

(*continued on p. 301*)

* The total energy of the electronic state with configuration q_i and parallel electron spins of the half-filled levels is calculated as follows:

$$E\{q_i\} = \sum_i q_i \epsilon_i - \sum_a J_a \langle S_a^2 \rangle \quad (1)$$

where *a* implies summation over all *d* elements and the average local spin values are estimated according to the formula

$$\langle S_a^2 \rangle = \frac{na}{2}\left(\frac{na}{2}+1\right)$$

where *na* is the effective number of unpaired *d*-electrons determined from Mulliken population analysis. The following dependence of *J*(Cr) from the effective configuration of the Cr atom is adopted (in eV):

$$J(s^q d^{4+x}) = 0.752 - 0.034q - (0.02695 - 0.0126q)x^2 - (0.10145 - 0.0044q)x$$

Its coefficients were found from the values of the Racah parameters $F^2(3d3d)_4 F^4(3d3d)$ in different configurations of the Cr atom [12]. The influence of *s* and *p* electrons on the *J* value is assumed to be equal: $J(d^n s^m p^k) = J(d^n s^{k+m})$

Table 7

Quantum chemical parameters (ionization potentials and exponents) for $Cp_2Cr_2(\mu\text{-}OCMe_3)_2(OCMe_3)_2$ (III)

Atom	AO	Ionization potential (eV)	Exponent
H	1*s*	13.6	1.3
C	2*s*	11.4	1.625
	2*p*	11.4	1.625
N	2*s*	26.0	1.95
	2*p*	13.4	1.95
O	2*s*	32.3	2.275
	2*p*	14.8	2.275
Cr	3*d*	11.22	4.95 (0.48761) [a]
			1.60 (0.72051) [a]
	4*s*	8.66	1.7
	4*p*	5.24	1.7

[a] Coefficients of linear combination of the normalized Slater AO for the bi-exponential basis functions are given in parentheses.

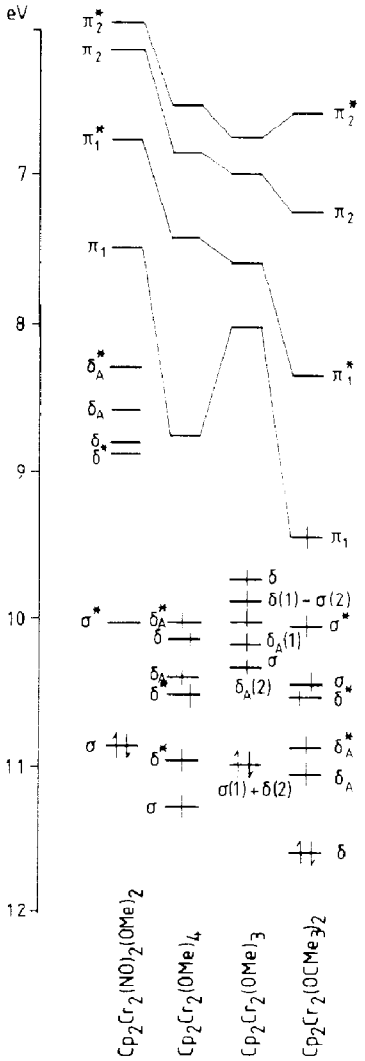

Fig. 3. Energy level diagram.

Table 8

Composition of the lowest energy *d*-type orbitals

	$(CpCr)_2(NO)_2(OMe)_2$ [a] (V)			$(CpCr)_2(OMe)_2(\mu\text{-}OMe)_2$ [a] (model of III)			$(CpCr)_2(OMe)(OMe)_2$ [a] (model of II)			$(CpCr)_2(OCMe_3)_2$ [a] (I)		
	A	B	C	A	B	C	A	B	C	A	B	C
σ	43.0	43.0	+0.0296	41.4	41.7	+0.324	31.0	49.7	+0.0064	37.0	42.2	+0.0281
$\sigma^\star$	40.0	40.0	−0.0467	52.7	28.4	−0.0278	46.5	41.2	−0.0425 [b]	46.7	43.8	−0.0742
δ_A	23.7	23.7	+0.0079	40.0	39.2	+0.0317	0.8	87.6	−0.0061	36.4	47.2	+0.0265
$\delta_A^\star$	24.5	24.5	−0.0129	44.0	39.5	−0.0641	73.4	0.8	−0.0045	51.5	39.5	−0.0401
δ	26.9	26.9	+0.0671	30.7	43.2	−0.0013	34.4	41.2	+0.0253	40.9	40.0	+0.0939
$\delta^\star$	33.5	33.5	−0.0850	31.8	47.6	−0.0057	35.9	47.2	+0.0528 [c]	39.8	41.4	−0.0150

[a] A = localization on the Cr(1) *d*-orbitals (%). B = localization on the Cr(2) *d*-orbitals (%). C = Contribution to the population of the Cr–Cr bond when the corresponding orbital contains one electron. [b] This is, in fact, the $\delta(Cr(1)) - \sigma(Cr(2))$ orbital. [c] This is, in fact, the $\sigma(Cr(1)) - \delta(Cr(2))$ orbital.

Table 9

Characteristics of the complexes in different spin states

	$Cp_2Cr_2(OMe)_2(NO)_2$ (V)		$Cp_2Cr_2(OMe)_2(OMe)_2$ (model of III)		$Cp_2Cr_2(OMe(OMe)_2$ (model of II)		$Cp_2Cr_2(OCMe_3)_2$ (I)	
A [a]	1/2	1/2	1	1	1	1/2	1/2	1/2
B	0.829	0.829	1.552	1.585	1.510	0.916	0.767	0.835
C	3.573/0.698	3.573/0.698	4.193/0.674	4.524/0.681	4.132/0.639	5.118/0.540	4.940/0.534	4.949/0.559
D	0.767		0.706		0.663		0.622	
E	0.827 − 0.899 = −0.072		0.590 − 1.975 = −1.385		0.367 − 1.314 = −0.947		0.074 − 0.698 = −0.625	
A			3/2	3/2	1	3/2	1	1
B			2.406	2.397	1.861	2.204	1.769	1.669
C			4.219/0.697	4.233/0.678	4.467/0.652	4.654/0.562	4.893/0.562	4.992/0.587
D			0.706		0.670		0.622	
E			1.853 − 3.730 = −1.877		1.308 − 2.714 = −1.406		0.888 − 1.966 = −1.077	
A					3/2	2	3/2	3/2
B					2.363	3.241	2.399	2.498
C					4.251/0.641	4.748/0.582	4.814/0.603	4.877/0.619
D					0.673		0.634	
					3.833 − 4.620 = −0.787		2.489 − 3.454 = −0.965	
A							2	2
B							3.191	3.224
C							4.787/0.623	4.802/0.586
D							0.640	
E							5.734 − 5.344 = +0.390	

[a] A = Local spins. B = Local densities of unpaired *d*-electrons. C = Local $d/(s + p)$ configurations. D = The mean J (eV) parameter. E = Energy = $E = J_0$ relative to the state with minimal local spins (eV). E and J_0 are the contributions of the first and second terms on the right-hand side of **1**, respectively.

Table 10

Magnetic properties of complexes I–III and V

Parameter	Cp_2Cr_2-(μ-$OCMe_3)_2$ (I)	$Cp_2Cr_2(\mu$-$OCMe_3)_2$ ·$OCCo_3(CO)_9$ (II)	$Cp_2Cr_2(OCMe_3)_2$-(μ-$OCMe_3)_2$ (III)	$Cp_2Cr_2(NO)_2$-(μ-$OMe)_2$ (V)
μ_{eff}. MB per Cr atom	1.88–1.49	2.48–1.72	2.83–1.40	diamagnetic
T (K)	333.5–214	296–79	295–79	296–77
S_A and S_B	3/2 3/2	1 3/2	3/2 3/2	1/2 1/2
$-2J$ (cm^{-1})	204	164	70	>1000
$-2J = 4S_AS_B \cdot -2J$ (cm^{-1})	1836	984	630	>1000

The value of the exchange parameter J in I is in good agreement with the existence of a strong single Cr–Cr bond in it, which is likely to be the main channel for exchange interactions. On the other hand, the $-2J$ value for III without any direct Cr–Cr bonding decreases considerably (to 70 cm^{-1}) and corresponds mainly to the indirect exchange via two alkoxide bridges. The picture becomes clearer if the values for the total exchange parameter $-2J$ are used for comparison [13] (Table 10);

$$-2J_{\Sigma} = -2J \cdot 4S_AS_B$$

The transition from complex III to V causes a decrease in spin to 1/2, which can result in diamagnetism of the complex at room temperature owing to the high value of J ($J = J_{\Sigma}$ in this case). As far as complex II with Cr atoms in different oxidation states is concerned, the $-2J$ and $-2J_{\Sigma}$ values correspond to the existence of a weak Cr–Cr bond; however, the observed μ_{eff} value (1.72 BM) at 79 K is somewhat higher than the expected value (in the case of strong exchange, this parameter should be equal to 1.22 BM per Cr atom). This fact may be due to the presence of small amounts of strongly paramagnetic impurities in the samples measured *, e.g. cobalt(II) oxide, since ESR measurements (performed on a large single crystal at 77 K) have revealed a singlet signal ($g = 2.0$) corresponding to one unpaired electron localized at the Cr^{II} atom.

Experimental

All operations connected with the synthesis of the initial complex I as well as complexes II–IV were conducted in a stream of pure argon; absolute solvents were used. I was obtained from Cp_2Cr and $HOCMe_3$ according to [1]. IR spectra were measured in KBr pellets or in suspension in nujol. ESR spectra were measured with a Sex-2542 instrument at 77 K. Magnetic susceptibility was measured according to the Faraday method, using the technique designed in the Institute of General and Inorganic Chemistry [14]. X-ray diffraction data were obtained with an automated Syntex $P2_1$ diffractometer (λ(Mo-K_α), $\theta/2\theta$ scan) at a temperature of $-100\,^{\circ}C$ for II, and with an automated Hilger & Watts diffractometer (λ(Mo-K_α), $\theta/2\theta$-scan, T $20\,^{\circ}C$) for III (Table 11). Structures II and III were solved by the direct method

* A series of independent measurements of large single crystals of II was carried out.

Table 11

Crystal data for complexes II and III

	$Cp_2Cr_2(\mu\text{-}OCMe_3)_2$-$[OCCo_3(CO)_9]$ (II)	$Cp_2Cr_2(OCMe_3)_2$-$(\mu\text{-}OCMe_3)_2$ (III)
Crystal system	monoclinic	orthorhombic
Space group	$P2_1/n$	$Pna2_1$
a (Å)	10.377(4)	22.4539(12)
b (Å)	17.879(7)	11.7514(6)
c (Å)	18.115(7)	10.7303(5)
β(°)	101.39(3)	
V (Å^3)	3294.7	2831.3
Z	4	4
$2\theta_{max}$	56	54
Number of reflections measured	6318	2723
Number of reflections with $I > 3\sigma$ used in refinement	5428	1801
R_1	0.044	0.070
R_w	0.048	0.072

using the MULTAN program and were refined by the block-diagonal least-squares technique in an anisotropic approximation for all non-hydrogen atoms. The hydrogen atoms in structure II were located in the difference Fourier synthesis; their contribution to F_{calc} was taken into account, but positional and thermal parameters were not refined. All calculations were carried out using the INEXTL program package [15] with an Eclipse S/200 computer.

Synthesis of $Cp_2Cr_2(\mu\text{-}OCMe_3)_2[\mu\text{-}OCCo_3(CO)_9]$ (II)

Addition of a solution of 0.93 g (2.7 mM) of $Co_2(CO)_8$ in 10 ml of benzene to a red-brown solution of $Cp_2Cr_2(\mu\text{-}OCMe_3)_2$ (obtained from 1 g (5.5 mM) of Cp_2Cr and Me_3COH) in 10 ml of benzene instantly yielded a crimson solution. This transparent solution was kept at +5°C for 2 days. The large brown-crimson crystals which precipitated from this solution were separated by decantation, washed with benzene/heptane (1/5 mixture) and dried at room temperature in an argon flow. The product was extremely sensitive to atmospheric oxygen and moisture.

Yield 0.61 g (27%) relative to Cp_2Cr. IR spectrum (Nujol) (ν, cm^{-1}): 2080m, 2015vs br, 1990s br, 1965m, 1880m, 1160m br, 810m, 775w, 720w, 670m, 605w, 560w, 500w, 450. IR spectrum (KBr) (ν, cm^{-1}): 2900w br, 2080m, 2000s br, 1455m, 1435m br, 1390m br, 1160w, 890w br, 800w, 660w, 550w, 500m br.

The product yield increased to 61% when the ratio of the components was 1/3.

Synthesis of $Cp_2Cr_2(\mu\text{-}OR)_2(OR)_2$ (III)

An excess of solid Te was added to a red-brown solution of $Cp_2Cr_2(\mu\text{-}OCMe_3)_2$ (obtained from 0.5 g (2.7 mM) of Cp_2Cr and Me_3COH) in 25 ml of toluene. The reaction mixture was refluxed for 2 h, the brown-green solution formed was filtered, and the solvent was then evaporated in an argon flow at 120°C. The solid residue was extracted by hot heptane until the solution became colourless (total amount

40–60 ml); a fine crystalline precipitate of $Cp_4Cr_4Te_4$ (IV) was left. The green heptane extract was concentrated at 120 °C in an argon flow to 5–8 ml and cooled to −15 °C. The large green prisms which precipitated from the solution in one day were isolated from the solution by decantation, washed with cold (−20 to −30 °C) heptane and dried in vacuo. The yield of $Cp_2Cr_2(\mu\text{-}OCMe_3)_2(OCMe_3)_2$ was 0.1 g (14% relative to Cp_2Cr).

IR spectrum (ν, cm^{-1}) 540m br, 575s, 780s, 790s, 880s, 980s, 1000w, 1170s br, 1335m, 1360w, 2920w br, 2950w br.

References

1 M.H. Chisholm, F.A. Cotton, M.W. Extine, P.C. Rideout, Inorg. Chem., 18 (1979) 120.
2 I.L. Eremenko, A.A. Pasynskii, Yu.V. Rakitin, O.G. Ellert, V.N. Novotortsev, V.T. Kalinnikov, V.E. Shklover, Yu.T. Struchkov, J. Organomet. Chem., 256 (1983) 291.
3 A.A. Pasynskii, I.L. Eremenko, Yu.V. Rakitin, V.M. Novotortsev, V.T. Kalinnikov, Yu.T. Struchkov, G.G. Aleksandrov, J. Organomet. Chem., 165 (1979) 57.
4 S.E. Nefedov, A.A. Pasynskii, I.L. Eremenko, B. Orazsakhatov, V.M. Novotortsev, O.G. Ellert, S.B. Katser, A.S. Antsyshkina, M.A. Porai-Koshits, J. Organomet. Chem., 345 (1988) 97.
5 P.W. Sutton, L.F. Dahl, J. Am. Chem. Soc. 89 (1967) 261.
6 I.P. Beletskaja, G.Z. Suleimanov, Metalloorganicheskaja Khim., 1 (1988) 10.
7 G. Schmid, B. Stutte, R. Boese, Chem. Ber., 111 (1978) 1239.
8 A.U. Hurdy, G.A. Sim, Acta Cryst. B, 35 (1979) 1463.
9 J.H. Ammeter, H.B. Bürge, J.C. Thibeault, R. Hoffmann, J. Am. Chem. Soc., 100 (1978) 3686.
10 I.L. Eremenko, A.A. Pasynskii, B. Orazsakhatov, A.F. Shestakov, G.Sh. Gasanov, A.S. Katugin, Yu.T. Struchkov, V.E. Shklover, J. Organomet. Chem., 338 (1988) 369.
11 J.H. Van Vleck, The Theory of Electronic and Magnetic Susceptibilities, Oxford Univ. Press, London, 1932.
12 P. Pelikán, R. Boča, M. Liška, L. Turi Nagy, Chem. Zvesti, (S) 32, (1978) 592.
13 M.V. Eremin, Yu.V. Rakitin, Phys. Stat. Sol. (b), 80 (1977) 579.
14 V.M. Novotortsev, Dr.Ph. Thesis, Moscow, 1974.
15 R.G. Gerr, A.I. Yanovsky, Yu.T. Struchkov, Kristallographia, 28 (1983) 1029.
16 I.L. Eremenko, S.E.. Nefedov, A.A. Pasynskii, B. Orazsakhatov, O.G. Ellert, Yu.T. Struchkov, A.I. Yanovsky, D.V. Zagorevsky, J. Organomet. Chem., 368 (1989) 185.